Supplemental Materials

Methylation in pericytes after acute injury promotes chronic kidney disease

Yu-Hsiang Chou, Szu-Yu Pan, Yu-Han Shao, Hong-Mou Shih, Shi-Yao Wei, Chun-Fu Lai, Wen-Chih Chiang, Claudia Schrimpf, Kai-Chien Yang, Liang-Chuan Lai, Yung-Ming Chen, Tzong-Shinn Chu, Shuei-Liong Lin

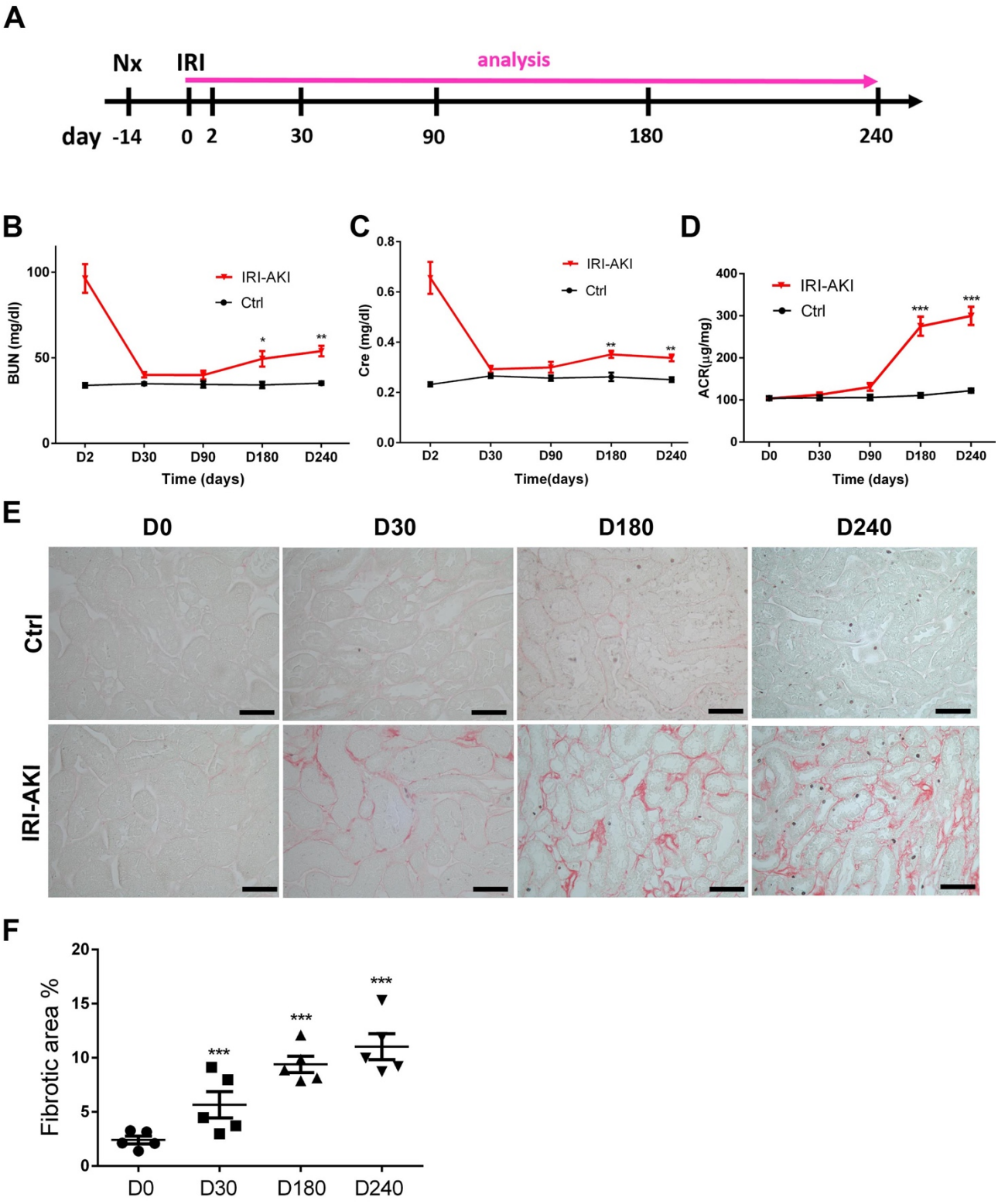

Supplemental Figure 1. A murine model of acute kidney injury–chronic kidney disease continuum. (A) Experimental scheme showing acute kidney injury (AKI) induced by left renal ischemia-reperfusion injury (IRI-AKI) 2 weeks after right nephrectomy (Nx). Plasma, urine and kidney were analyzed at the indicated time points. **(B, C, D)** Line charts showing the plasma blood

urea nitrogen (BUN), creatinine (Cre) and urine albumin-creatinine ratio (ACR) at the indicated time points. Mice with Nx only served as the control (Ctrl). Data were expressed as the mean ± SEM. *P<0.05, **P<0.01, ***P<0.001 vs. Ctrl at the indicated time points (D indicates day) by t-test. n=5. **(E)** Representative images showing picrosirius red staining in the kidneys at the indicated time points. Scale bar, 50 μm. **(F)** Dot chart showing the quantification of picrosirius red-stained fibrotic area (%) in the kidneys at the indicated time points. Horizontal bars represent the mean, error bars represent the SEM. **P<0.01, ***P<0.001 vs. Ctrl on D0 by one-way ANOVA with post hoc Dunnett's correction. n=5.

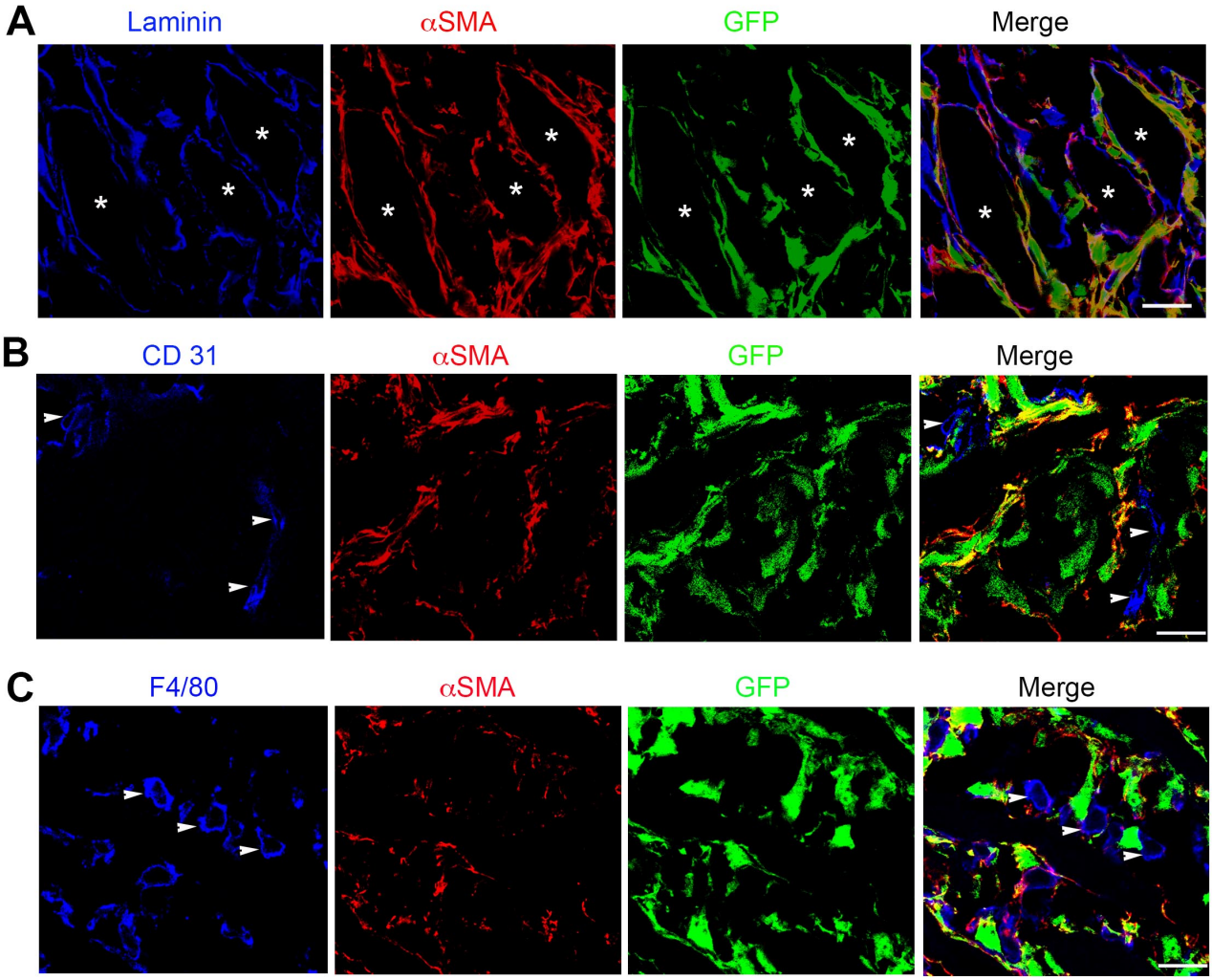

Supplemental Figure 2. Cellular specificity of αSMA$^+$Col1a1-GFP$^+$ myofibroblasts. Representative images showing the cell marker staining of αSMA$^+$Col1a1-GFP$^+$ myofibroblasts in the kidneys of *Col1a1-GFP^{Tg}* mice on day 7 after IRI-AKI. **(A)** Laminin staining for the tubular basement membrane. Representative images showing that αSMA$^+$Col1a1-GFP$^+$ myofibroblasts did not co-localize with tubular epithelial cells who were enclosed within the laminin$^+$ tubular basement membrane. Asterisks indicate the renal tubular lumen. **(B)** CD31 staining for the endothelial cells. Representative images showing that αSMA$^+$Col1a1-GFP$^+$ myofibroblasts did not co-localize with the CD31$^+$ endothelial cells. Arrows indicate CD31$^+$ endothelial cells. **(C)** F4/80 staining for the macrophages. Representative images showing that αSMA$^+$Col1a1-GFP$^+$ myofibroblasts did not co-localize with the F4/80$^+$ macrophages. Arrows indicate the F4/80$^+$ macrophages. Scale bar, 25 μm. Original magnification, 400X.

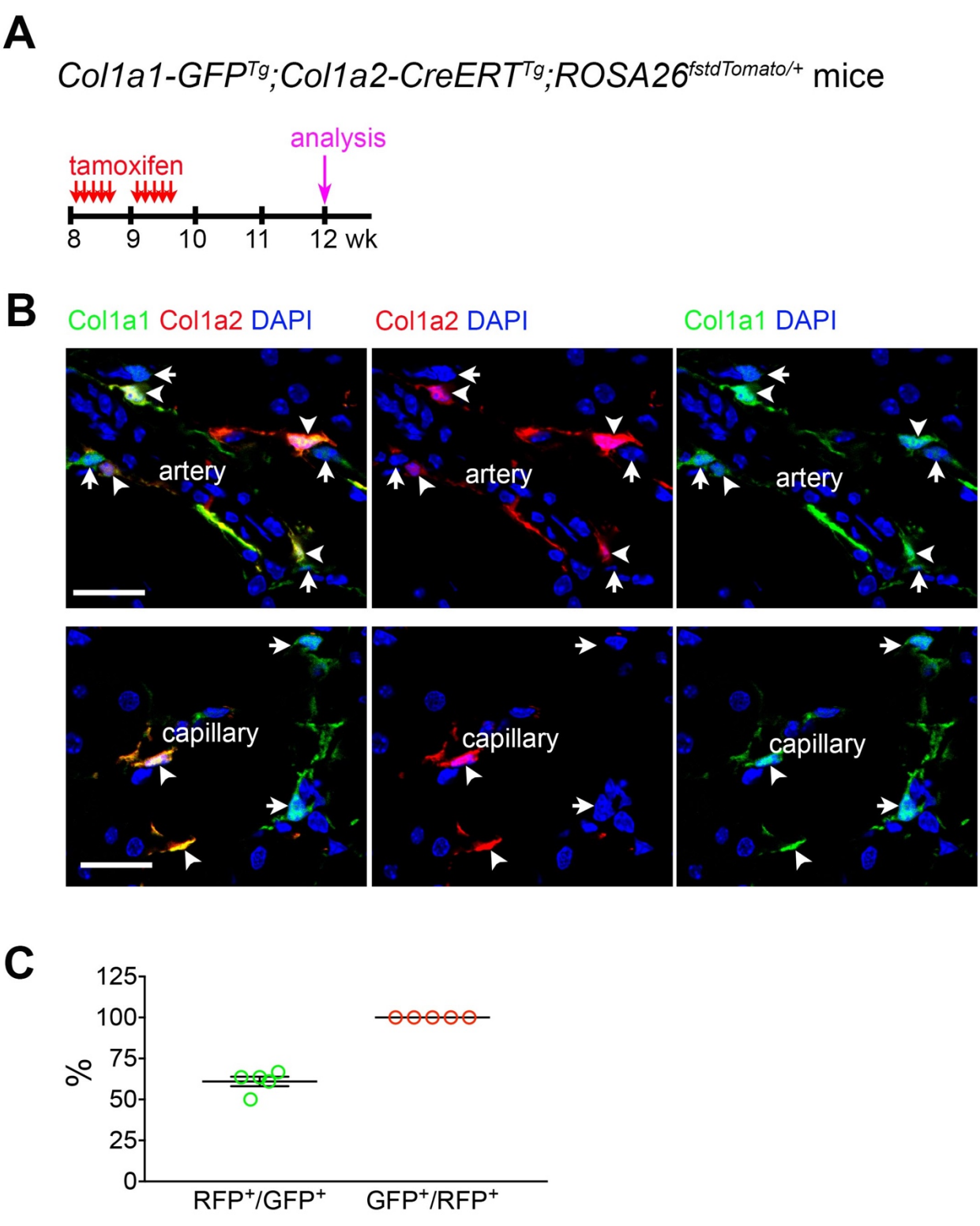

Supplemental Figure 3. All Col1a2-RFP^{+} cells were Col1a1-GFP^{+} pericytes in *Col1a2-CreERT^{Tg};ROSA26$^{fstdTomato/+}$* mice. **(A)** Experimental scheme for tamoxifen-induced expression of tdTomato red fluorescence protein (RFP) in *Col1a2*-expressing pericytes. **(B)** Representative images showing co-localization of Col1a2-RFP and Col1a1-GFP in the kidney pericytes. Arrows and

arrowheads indicate Col1a1-GFP$^+$ pericytes and Col1a1-GFP$^+$Col1a2-RFP$^+$ pericytes, respectively. Scale bar, 50 μm. **(C)** Dot chart showing the percentage of Col1a1-GFP$^+$ pericytes with Col1a2-RFP expression (RFP$^+$/GFP$^+$) and the percentage of Col1a2-RFP$^+$ pericytes with Col1a1-GFP expression (GFP$^+$/RFP$^+$). Horizontal bars represent the mean, error bars represent the SEM. *n*=5.

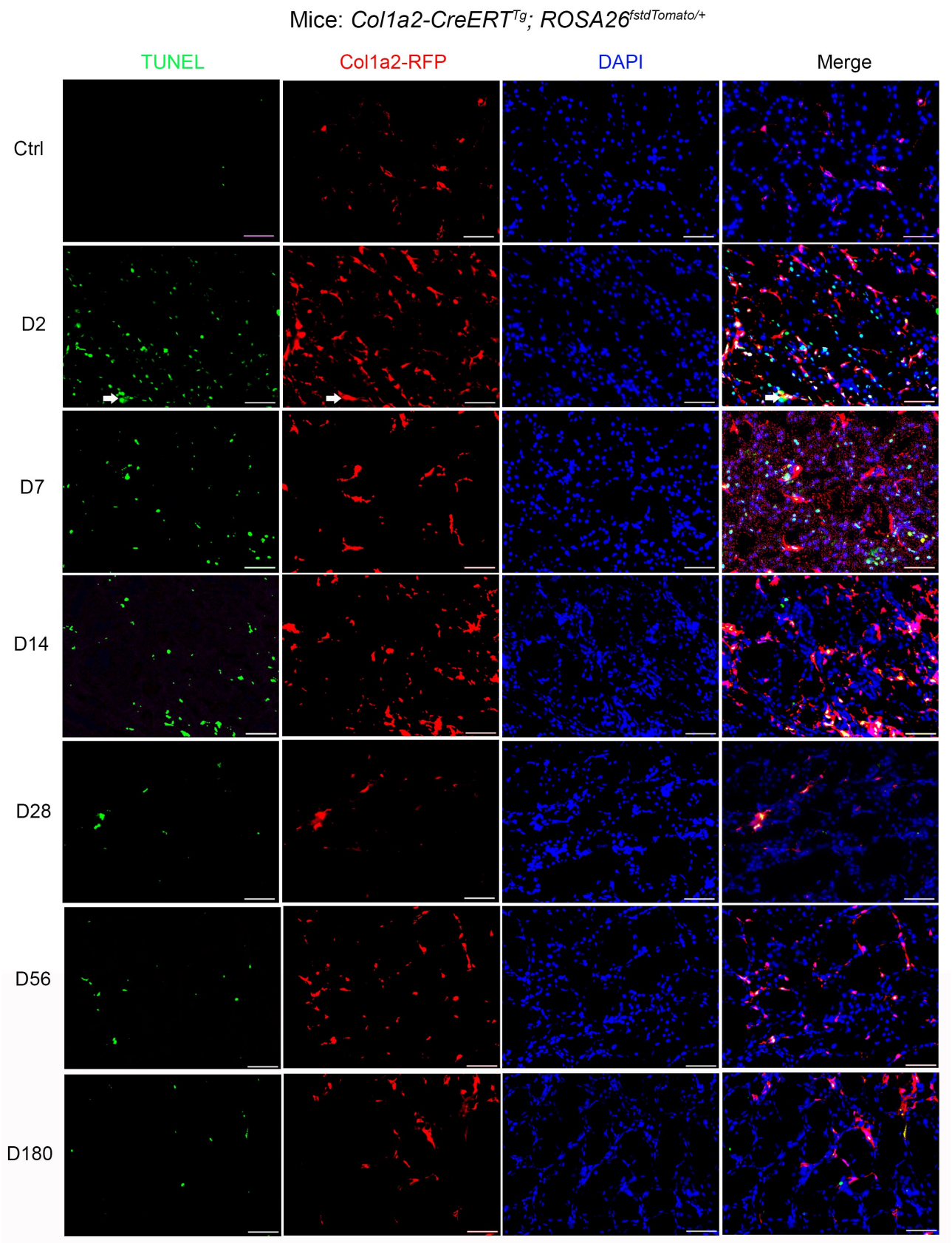

Supplemental Figure 4. Col1a2-RFP$^+$ pericytes apoptosed after acute kidney injury. Representative images showing Col1a2-RFP$^+$ pericytes and terminal deoxynucleotidyl transferase dUTP nick end labeling (TUNEL) staining in the kidneys at the indicated time points after IRI-AKI.

The normal kidney at D0 was used as the Ctrl. Arrows indicate $TUNEL^{+}Col1a2\text{-}RFP^{+}$ pericytes. Scale bar, 50 μm.

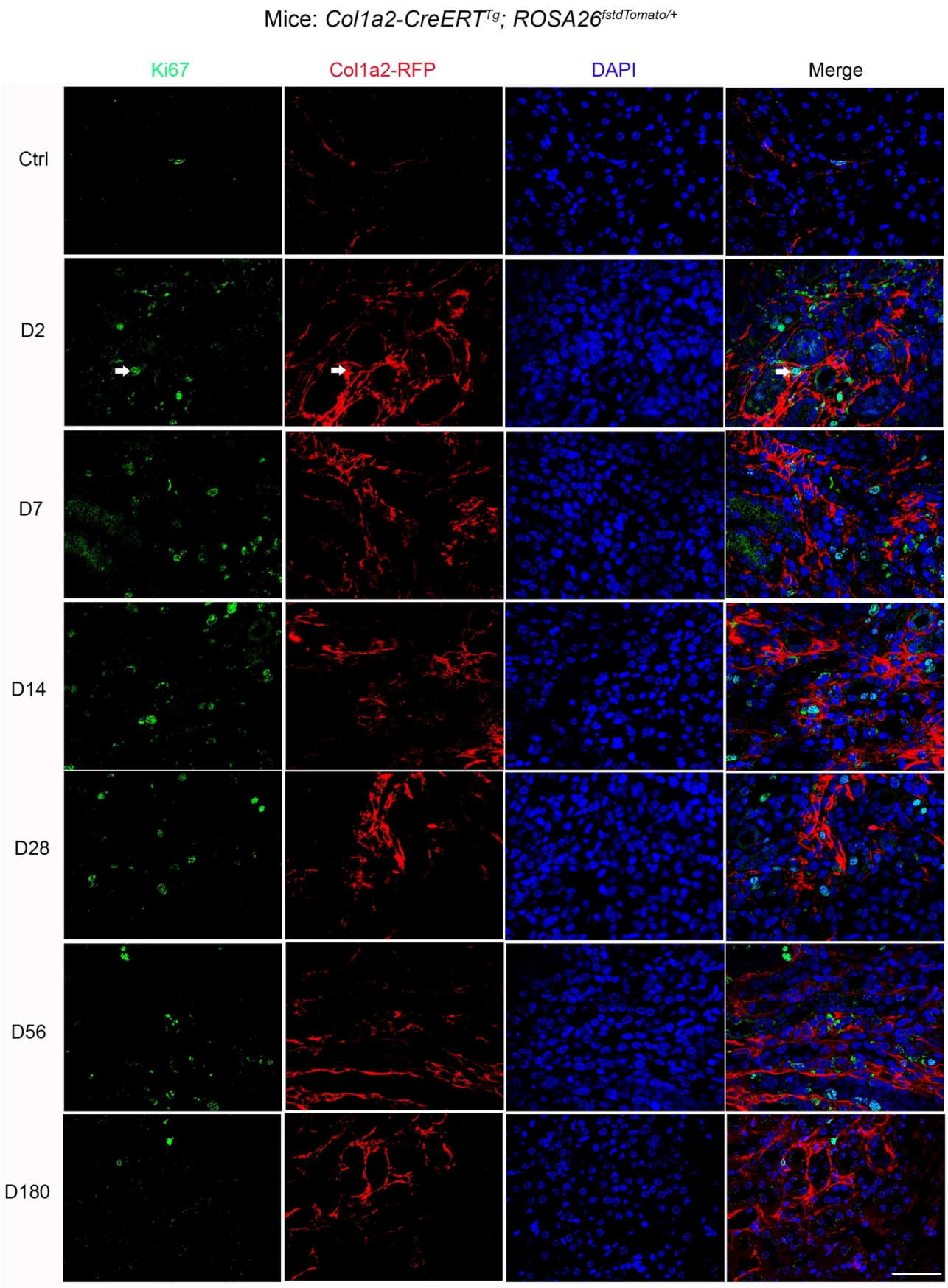

Supplemental Figure 5. Col1a2-RFP$^+$ pericytes proliferated after acute kidney injury. Representative images showing Col1a2-RFP$^+$ pericytes and Ki67$^+$ staining in the kidneys at the

indicated time points after IRI-AKI. The normal kidney at D0 was used as the Ctrl. Arrows indicate $Ki67^{+}Col1a2\text{-}RFP^{+}$ pericytes. Scale bar, 50 μm.

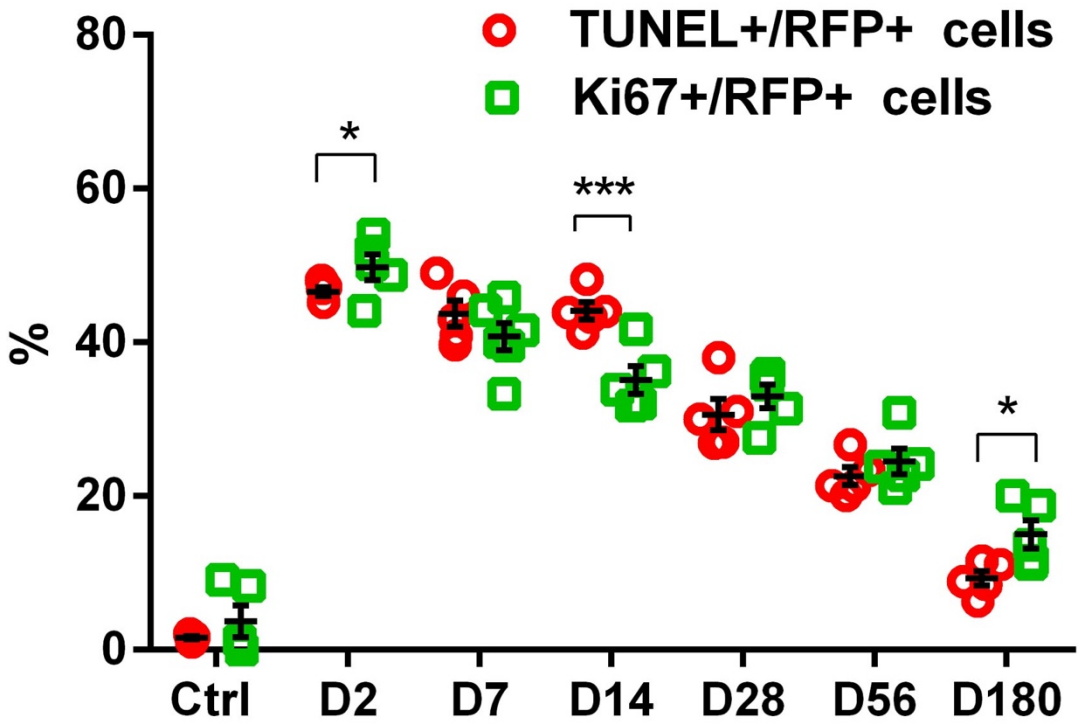

Supplemental Figure 6. Apoptosis outweighed cell proliferation in Col1a2-RFP$^+$ pericytes in the stage of acute kidney disease. Dot chart showing the percentage of Col1a2-RFP$^+$ pericytes with TUNEL$^+$ or Ki67$^+$ staining at the indicated time points after IRI-AKI. The quantification was derived from the results in Supplemental Figure 4 and 5. The period between day 7 and 90 after IRI-AKI was in the stage of acute kidney disease. Horizontal bars represent the mean, error bars represent the SEM. *P<0.05, ***P<0.001 by t-test. n=5.

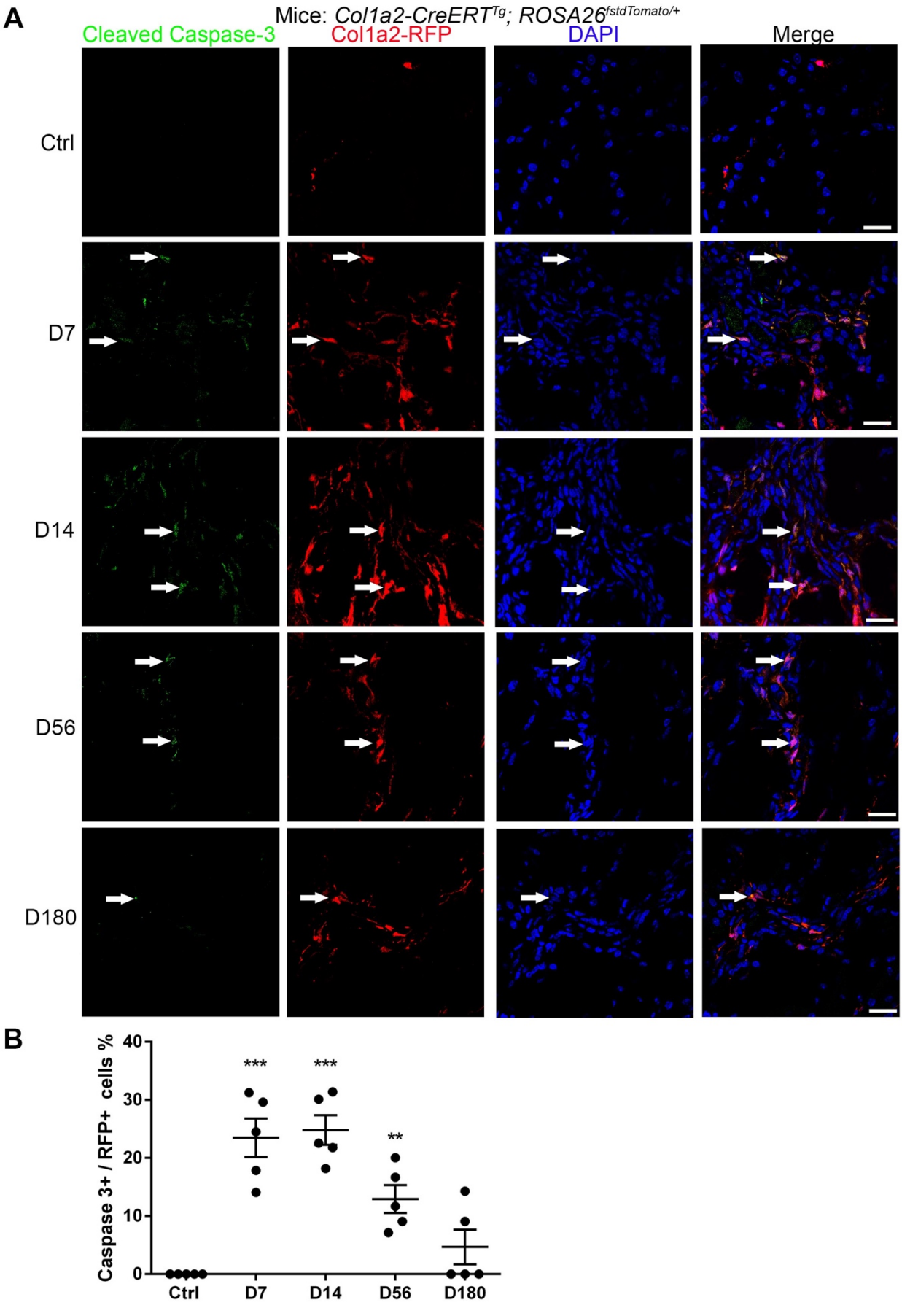
A
Mice: Col1a2-CreERT^Tg; ROSA26^fstdTomato/+
Cleaved Caspase-3
Col1a2-RFP
DAPI
Merge
Ctrl
D7
D14
D56
D180
B
Caspase 3+ / RFP+ cells %
40
30
20
10
0
***
***
**
Ctrl
D7
D14
D56
D180

Supplemental Figure 7. Col1a2-RFP$^+$ pericytes apoptosed after acute kidney injury. (A) Representative images showing Col1a2-RFP$^+$ pericytes and cleaved caspase-3 staining in the kidneys at the indicated time points after IRI-AKI. The normal kidney at D0 was used as the Ctrl. Arrows indicate cleaved caspase-3$^+$Col1a2-RFP$^+$ pericytes. Scale bar, 50 μm. **(B)** Dot chart showing the percentage of Col1a2-RFP$^+$ pericytes with cleaved caspase-3$^+$ staining. Horizontal bars represent the mean, error bars represent the SEM. ***P*<0.01, ****P*<0.001 vs. Ctrl by one-way ANOVA with post hoc Dunnett's correction. *n*=5.

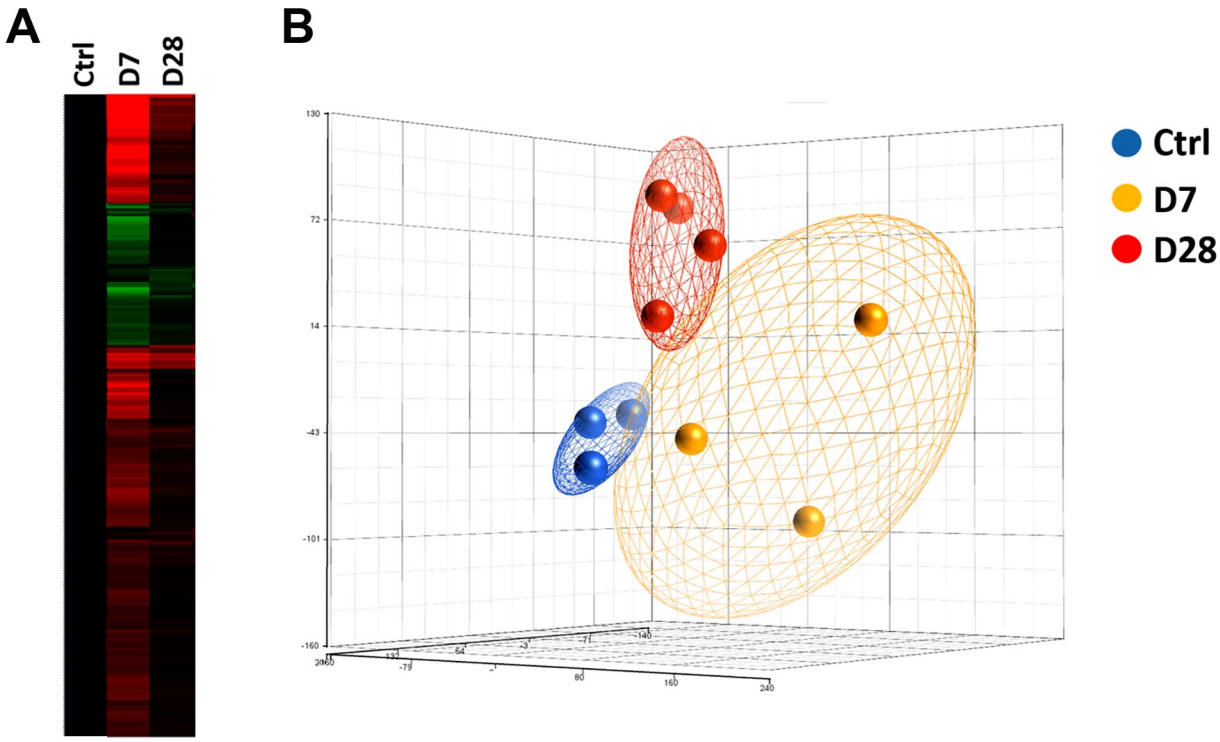

Supplemental Figure 8. Heatmap and principal component analysis of microarray data demonstrated distinctive gene expression of pericytes at the indicated time points. Purified pericytes by sorting $RFP^{+}GFP^{+}F4/80\text{-}APC^{-}CD31\text{-}APC^{-}CD324\text{-}APC^{-}$ cells from *Foxd1*$^{Cre/+}$;*ROSA26*$^{fstdTomato/+}$;*Col1a1-GFP*^{Tg} mice at the indicated time points after IRI-AKI were used for whole-genome microarrays. The normal kidney pericytes at D0 was used as the Ctrl. **(A)** Heatmap of microarray data of the pericytes at the indicated time points. **(B)** Three-dimensional plot of principal component analysis (PCA) showing distinctive cluster of genes expressed in the pericytes sorted at the indicated time points.

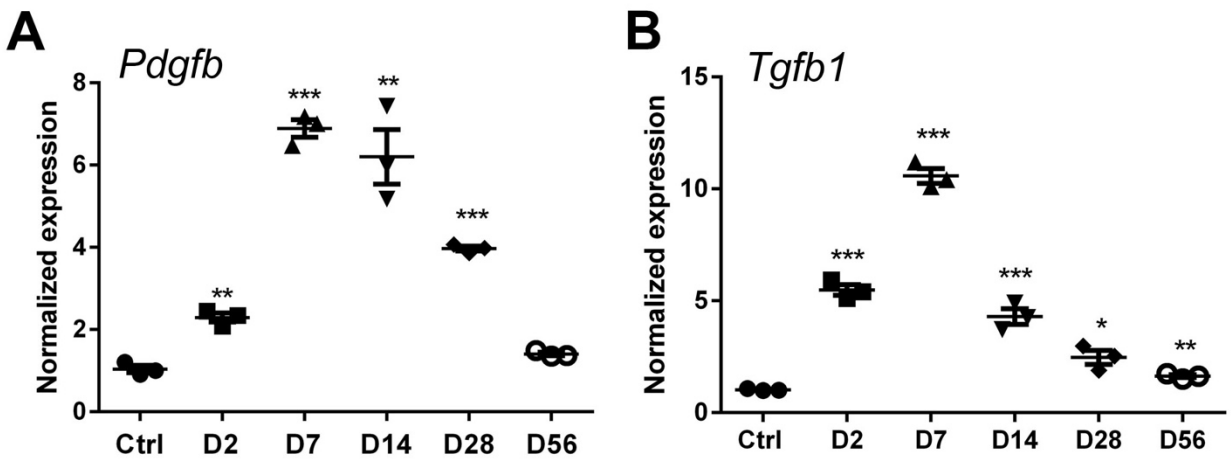

Supplemental Figure 9. Transient increase of key growth factors for pericytes in the kidney after acute kidney injury. Dot charts showing the quantitative PCR time course for the transcripts of renal *Pdgfb* and *Tgfb1* at the indicated time points. The normal kidney at D0 was used as the Ctrl. *Pdgfb* and *Tgfb1* encode platelet-derived growth factor-B and transforming growth factor-β1 (TGF-β1), respectively. Horizontal bars represent the mean, error bars represent the SEM. **P*<0.05, ***P*<0.01, ****P*<0.001 versus Ctrl by one-way ANOVA with post hoc Dunnett's correction. *n*=3.

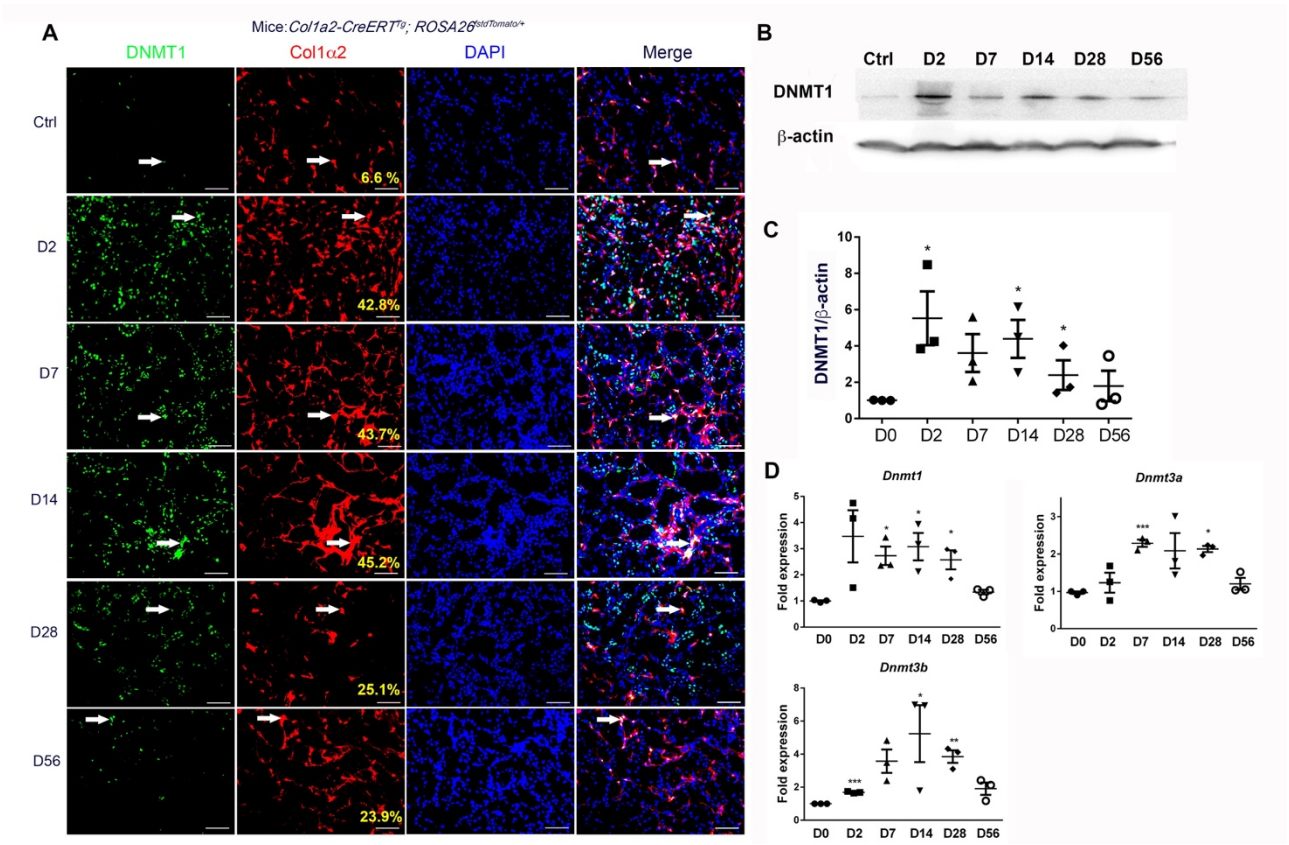

Supplemental Figure 10. DNA methyltransferase 1 increased in pericytes after acute kidney injury. (A) Representative images showing Col1a2-RFP^{+} pericyte lineage and DNA methyltransferase 1 (DNMT1)$^{+}$ cells in the kidneys at the indicated time points after IRI-AKI. The normal kidney at D0 was used as the Ctrl. Arrows indicate Col1a2-RFP^{+}DNMT1^{+} pericytes. The figures indicate the percentages of Col1a2-RFP^{+} pericytes with DNMT1 expression. Scale bar, 50 μm. Original magnification, 400X. **(B)** Representative images for the western blot analysis of renal DNMT1 and β-actin at the indicated time points. **(C)** Dot chart showing the relative expression of renal DNMT1 at the indicated time points. The expression of DNMT1 was normalized to β-actin. *n*=3. **(D)** Dot charts showing the quantitative PCR time course for the transcripts of renal *Dnmt1, Dnmt3a, Dnmt3b* at the indicated time points. *n*=3. Horizontal bars represent the mean, error bars represent the SEM. **P*<0.05, ***P*<0.01, ****P*<0.001 vs. Ctrl at D0 by one-way ANOVA with post hoc Dunnett's correction.

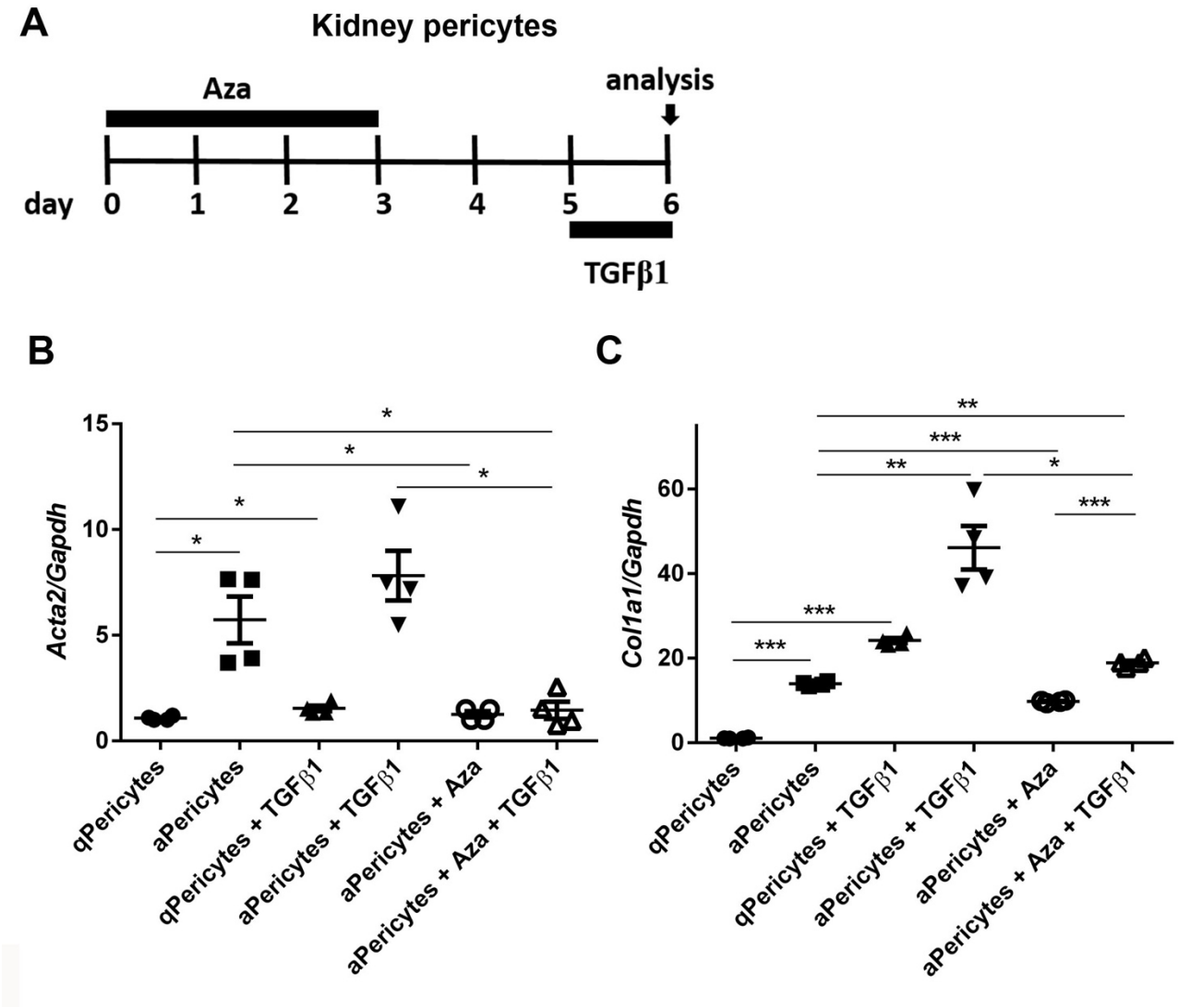

Supplemental Figure 11. Demethylation by 5-azacytidine prevented the profibrotic activities of myofibroblasts stimulated by transforming growth factor-β1. (A) Experimental scheme showing the stimulation of pericytes by TGF-β1 after 3-day exposure to 5-azacytidine (Aza) or vehicle. Quiescent pericytes (qPericytes) isolated from the normal kidneys and activated pericytes (aPericytes, myofibroblasts) isolated from the kidneys on day 7 after IRI-AKI were used for experiments. **(B, C)** Dot charts showing the relative expression of *Acta2* and *Col1a1* induced by TGF-β1 in qPericytes and aPericytes/myofibroblasts in the presence or absence of Aza pretreatment. Horizontal bars represent the mean, error bars represent the SEM. **P*<0.05, ***P*<0.01, ****P*<0.001 by one-way ANOVA with post hoc Tukey's correction. *n*=4.

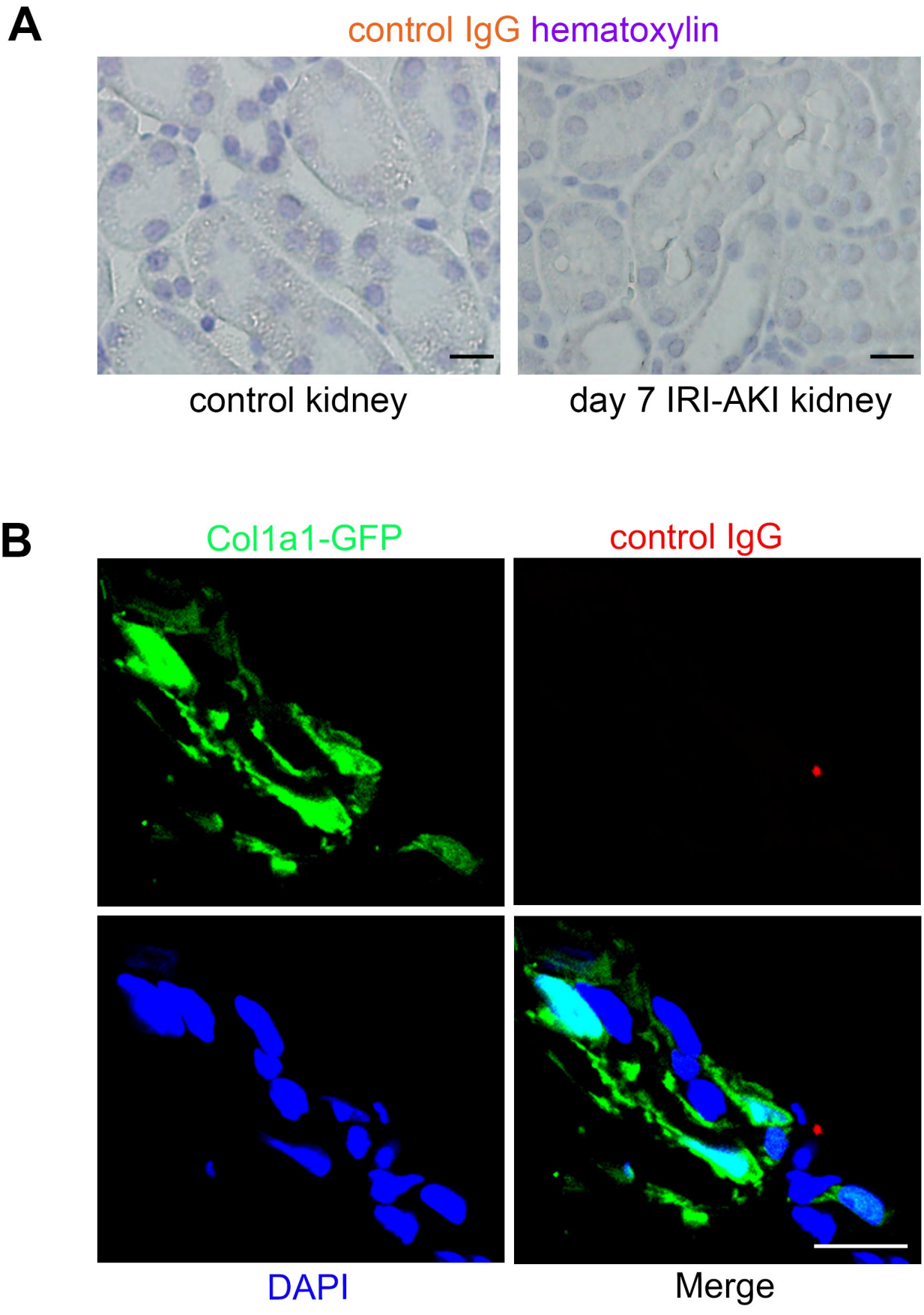
A
control IgG hematoxylin
control kidney
day 7 IRI-AKI kidney
B
Col1a1-GFP
control IgG
DAPI
Merge

Supplemental Figure 12. Negative control for YBX2 staining. (A) Representative images showing the immunohistochemistry staining using non-immunized rabbit IgG as the primary antibody in the kidneys. No specific staining was noted. **(B)** Representative images showing Col1a1-GFP^{+} pericytes in the normal control kidney of *Col1a1-GFP^{Tg}* mice. Immunostaining using non-immunized rabbit IgG followed by incubation with Cy3-conjugated goat anti-rabbit IgG antibody was performed. No specific Cy3 fluorescence was detected in the Col1a1-GFP^{+} pericytes. Scale bar, 25 μm. Original magnification, 400X.

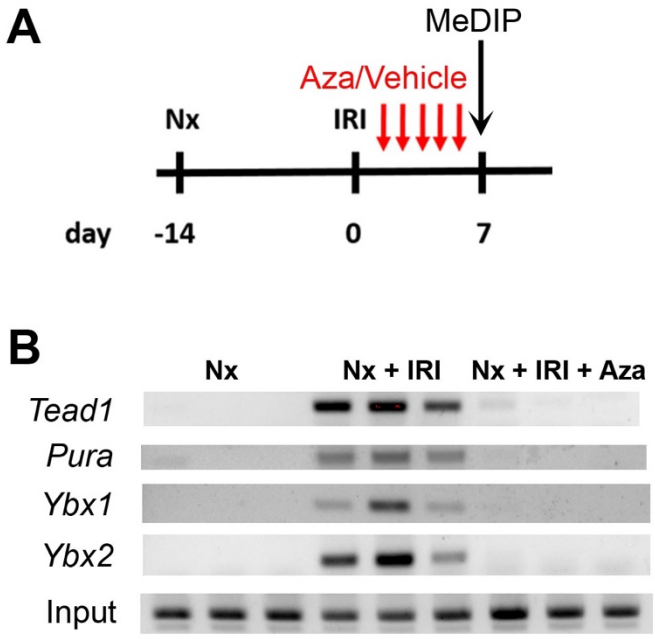

Supplemental Figure 13. Acute kidney injury resulted in methylation of *Tead1*, *Pura*, *Ybx1*, *Ybx2* genes in pericytes. (A) Experimental scheme for IRI-AKI and 5-azacytidine (Aza) treatment. Nx followed by sham operation served as the Ctrl. **(B)** Representative images showing the electrophoresis of PCR products for *Tead1, Pura, Ybx1* and *Ybx2* using immunoprecipitated methylated DNA (MeDIP) from the purified pericytes sorted from the kidneys on day 7 after IRI-AKI. Input DNA was used for *Gapdh* promoter PCR to confirm equal DNA in immunoprecipitation.

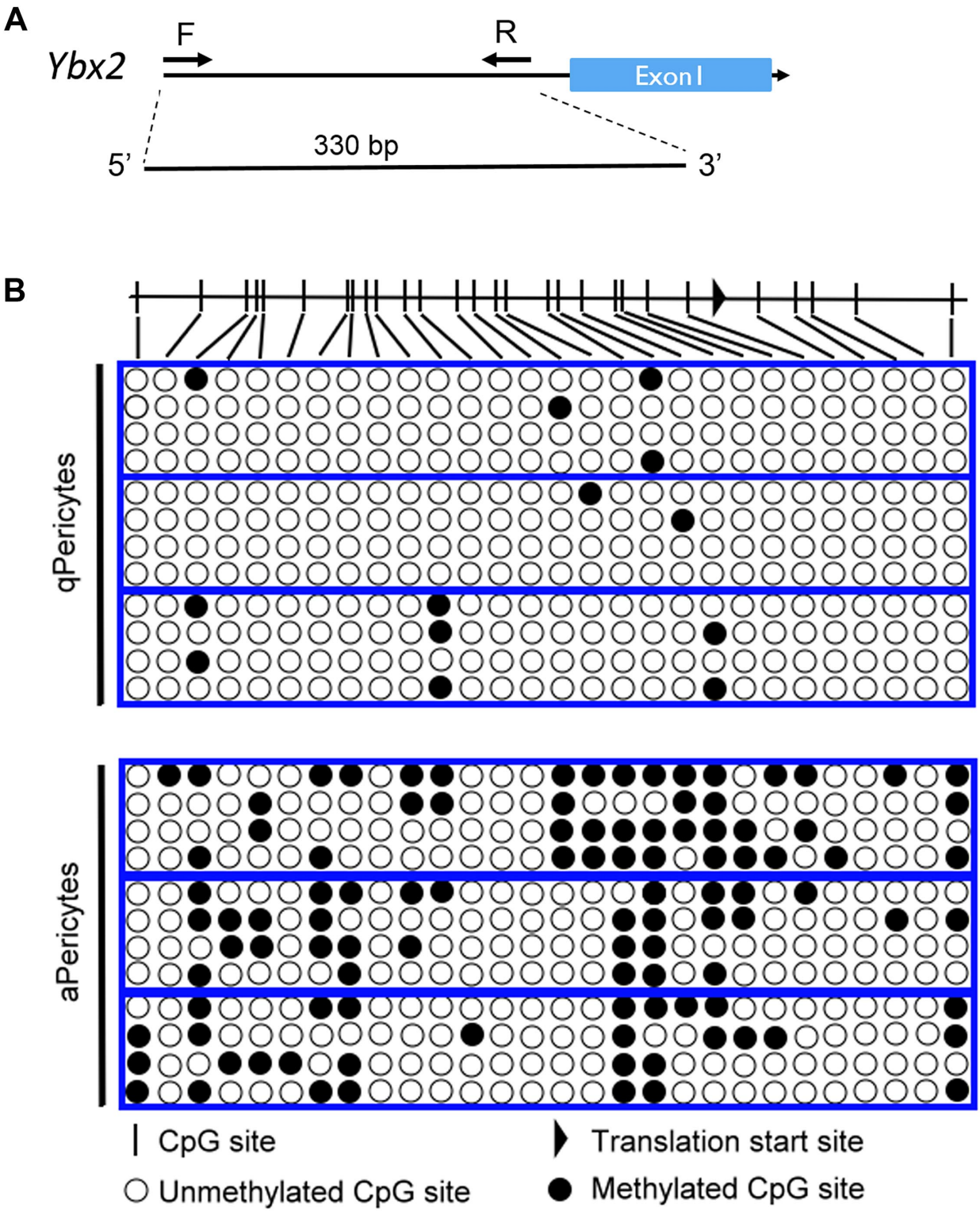

Supplemental Figure 14. Hypermethylation of *Ybx2* promoter in aPericytes after acute kidney injury. (A) Scheme for bisulfite genomic sequencing (BGS) illustrated the locations of PCR primers (forward and reverse for amplifying bisulfite-converted genomic DNA within the *Ybx2* promoter). **(B)** BGS of *Ybx2* promoter of purified qPericytes sorted from the normal kidneys and aPericytes sorted from the kidneys on day 7 after IRI-AKI. Each box represents the bisulfite genomic sequence

of the indicated cells isolated from one *Col1a1-GFP*^{Tg} mouse; each row represents a single sequenced clone (4 clones from each mouse); and each dot represents a single CpG.

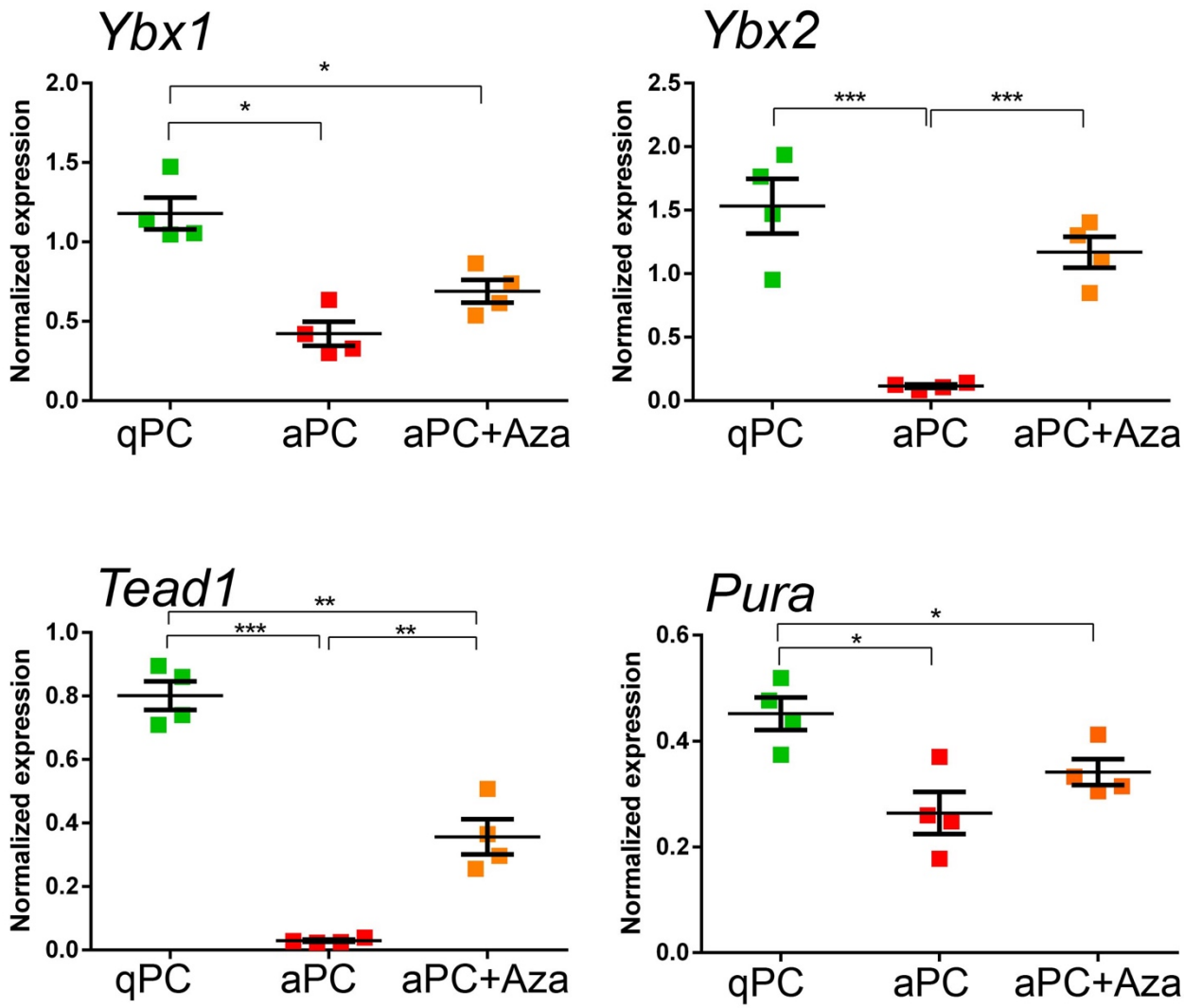

Supplemental Figure 15. The repression of *Tead1, Pura, Ybx1* and *Ybx2* genes in pericytes after acute kidney injury was reversed by demethylation. Pericytes were sorted from the kidneys of mice before (qPericytes, qPC) and on day 7 after IRI-AKI without (aPericytes, aPC) or with 5-azacytidine treatment (aPC+Aza) according to the experimental scheme shown in Supplemental Figure 13A. Dot charts showing the quantitative PCR results of *Tead1*, *Pura*, *Ybx1*, and *Ybx2* in the indicated pericytes. Expression was normalized to *Gapdh*. Horizontal bars represent the mean, error bars represent the SEM. **P* <0.05, ***P*<0.01, ****P* <0.001 by one-way ANOVA with post hoc Tukey's correction. *n*=4.

Supplemental Table 1. Primer sequences used in quantitative polymerase chain reaction

Gene		Sequence
Acta2	Forward	5’-CTG ACA GAG GCA CCA CTG AA-3’
	Reverse	5’-CAT CTC CAG AGT CCA GCA CA-3’
Col1a1	Forward	5’-GAG CGG AGA GTA CTG GAT CG-3’
	Reverse	5’-GTT CGG GCT GAT GTA CCA GT-3’
Col3a1	Forward	5’-ACC AAA AGG TGA TGC TGG AC-3’
	Reverse	5’-GAC CTC GTG CTC CAG TTA GC-3’
Timp1	Forward	5’-TGA TAG CTT CCA GTA AGG CC-3’
	Reverse	5’-CGA GAC CAC CTT ATA CCA GC-3’
Dnmt1	Forward	5’-CGG CTC AAA GAC TTG GAA AG-3’
	Reverse	5’-TAG CCA GGT AGC CTT CCT CA-3’
Dnmt3a	Forward	5’-ACC AGG CCA CCT ACA ACA AG-3’
	Reverse	5’-TGC TTG TTC TGC ACT TCC AC-3’
Dnmt3b	Forward	5’-ACT TGG TGA TTG GTG GAA GC-3’
	Reverse	5’-CCA GAA GAA TGG ACG GTT GT-3’
Tead1	Forward	5’-TAC TGC CAT CCA CAA CAA GC-3’
	Reverse	5’-TGC TGC ACA AAG GGC TTG AC-3’
Pura	Forward	5’-GAG AGT GGC TGA CTG GCT GT-3’
	Reverse	5’-GTC TCG GTC CGC CAT GAT-3’
Ybx1	Forward	5’-GGG ATC GGA AAG CGC TCC TG-3’
	Reverse	5’-CTT GCT CTC CTG CAC CCT GG-3’
Ybx2	Forward	5’-GAG TGT TGG AGA TGG GGA GA-3’
	Reverse	5’-CAG GTT CTG TCC CAC CTG AG-3’
Gapdh	Forward	5’-ACG GCC GCA TCT TCT TGT GCA-3’
	Reverse	5’-AAT GGC AGC CCT GGT GAC CA-3’
Angpt1	Forward	5'-GGA ACC GAG CCT ACT CAC AG-3'
	Reverse	5'-TTA GAT TGG AAG GGC CAC AG-3'
Angpt2	Forward	5'-CCG CTA CGT GCT TAA GAT CC-3'
	Reverse	5'-ATT GTC CGA ATC CTT TGT GC-3'
Timp3	Forward	5'-AGG GCC TCA ATT ACC GCT AC-3'
	Reverse	5'-GCG TTG CTG ATG CTC TTG TC-3'

Supplemental Table 2. Primer sequences used in regular polymerase chain reaction

Gene		Sequence
Promoter of *Acta2* (Region 1)	Forward	5'-GGC AAC ACA GGC TGG TTA AT-3'
	Reverse	5'-TAA GGA AGG GCC TGT CTC TG-3'
Promoter of *Acta2* (Region 2)	Forward	5'-GCC CTT CCT TAT CCA AGT CC-3'
	Reverse	5'-CTC TGT TCT GCT CCC GAA AC-3'
Promoter of *Acta2* (Region 3)	Forward	5'-GTT TCG GGA GCA GAA CAG AG-3'
	Reverse	5'-GCT GAA CGC TGA AGG GTT AT-3'
Promoter of *Ybx2,* for BGS	Forward	5'-GTT TTG TGT GGG AAG GTA TTT AGG G-3'
	Reverse	5'-TAA ATA CAC CTA AAC CCC ACC TCC CC-3'
Promoter of *Tead1*, for MeDIP	Forward	5'-CGA ACT TGG GTA AAG CGA AA-3'
	Reverse	5'-TAC TAG GAA TGC CGG GTG TG-3'
Promoter of *Purα*, for MeDIP	Forward	5'-AGG CCC TTA ACG CAG AGC-3'
	Reverse	5'-CTC GTT GCT GCC TCA CAC-3'
Promoter of *Ybx1*, for MeDIP	Forward	5'-CAA GGT GAC TGG ATC ACC AA-3'
	Reverse	5'-CGC CAT AGA GAC CGG AAC TA-3'
Promoter of *Ybx2*, for MeDIP	Forward	5'-CTT GCG CAC AGA AAC CAG-3'
	Reverse	5'-CTC CCG CAA CTC CGT AAG TA-3'
Promoter of *Gapdh*, for MeDIP	Forward	5'-GGT TAT CAC CAG GCC AGC TA-3'
	Reverse	5'-GGA AGG GAG AAA AGG CAT TC-3'